ISSN NO. 2320-5407

Journal homepage: http://www.journalijar.com

INTERNATIONAL JOURNAL OF ADVANCED RESEARCH

RESEARCH ARTICLE

The Influence of Doped-Kaolin on the Properties of Styrene-Butadiene Rubber Composites

Nivin M. Ahmed* and Salwa H. El-Sabbagh
Polymers and Pigments Department, National Research Centre, Dokki, Cairo, Egypt

Manuscript Info

Manuscript History:

Received: 15 March 2015
Final Accepted: 18 April 2015
Published Online: May 2015
Key words:

Corresponding Author

Nivin M. Ahmed

Abstract

Nowadays rubber-clay composites are spreading due to their high performance, cheap cost, high tensile strength and thermal stability. Kaolin is alumino-silicate clay which contains ɣ-alumina in its natural structure. In this study, doping process using ammonium molybdate was held on kaolin to convert ɣ-alumina naturally found in it to α-alumina which is a more stable phase that is not affected by the surrounding medium. Both kaolin and doped-kaolin were included in styrene-butadiene rubber (SBR) composites to study the cure characteristics, morphology, mechanical and thermal properties of these composites. SBR containing doped-kaolin showed improved properties than those containing kaolin due to the change in the filler particle size which is smaller in case of doped-kaolin, leading to higher homogeneity of filler dispersion in SBR which accordingly caused a change in the properties of SBR/doped-kaolin composites.

INTRODUCTION

The use of filler has played a vital role in rubber industry; the main purpose of adding fillers to polymers was primarily to improve mechanical properties and reduce cost. However, in recent years fillers are used often to fulfil a functional role such as increasing stiffness or improving the dimension stability of the polymer (Hernandezet al., 2007). The fillers used in polymers are usually kaolin, talc, silica, and calcium carbonate and to a lesser extent mica and wollastonite (Conceicao et al., 2003). The properties of filled polymers depend mainly on many factors including the properties of the matrix and filler, concentration and interactions of the different components (Markovic and Samarzija, 2010). In general, fillers lead to these improvements depend mainly on the choice of their origin, fraction, particle size, and surface treatment promoting interaction between the polymer matrix and the filler Panda et al., 2010).

Styrene-butadiene rubber (SBR) is widely used as one of the components of the elastomeric matrix for automotive tires, wire and cable applications due to its high fracture elongation, but unfortunately it has low elastic modulus and durability. In other word, SBR is not smooth or homogeneous and has poor physical properties, which means that it needs some additives such as; antioxidants, accelerators, softeners and fillers to improve its properties

Kaolin is clay that is widely used in various applications, such as ceramics, paper coating and filling, paint extender, rubber and plastic filler. It has major mineral component “Kaolinite” which usually contains quartz and mica (Ahmed, 2013). Chemically structured kaolin achieves its unique particle structure and size distribution through a carefully controlled proprietary steps, including doping of kaolin with different concentrations of ammonium molybdate that helps in converting alumina found naturally in kaolin from γ-alumina to α-alumina which is a more stable phase known as “corundum”, that is not affected by the surrounding media giving stiffness to the matrix leading to higher withstanding to mechanical stresses and other physical properties (Johns et al., 1990).

In this work, different concentrations of ammonium molybdate as dopant were added to kaolin to change the phase of alumina inside it, and then both kaolin and doped-kaolin were employed as reinforcing fillers in styrene butadiene rubber (SBR) composites. Rheometric, mechanical and thermal properties of the formed composites were

evaluated to point out the best concentration of dopant that can lead to better properties of the composites and the optimum loading of these fillers in SBR that can lead to higher performance composites.

2. Experimental

2.1. Materials and experimental techniques

2.1.1. Materials

- **SBR i**s styrene butadiene rubber (1502) with 23.5% styrene content, molecular weight M_W 140000g/mole, Mooney viscosity $M_L(1+4)$ at 100°C= 52 ± 3, and glass transition T_g = -60°C was purchased from Transport and Engineering Company (TRENCO) Alexandria.
- **Accelerators:** N-cyclohexyl-2-benzothiazole sulphen-amide (CBS), is pale grey powder with density 1.27-1.31 g/cm^3 at room temperature (25°C ± 1), melting point 95-100°C and its trade name is: Rhenogran® CBS-80, Vulkacit®CZ was bought from Rheinehemie Germany.
- **Antioxidants:** polymerized 2, 2, 4-trimethyl-1, 2-dihydroquinoline (TMQ), Trade name: PILnox® TDQ was obtained from NOCIL LIMITED Navi Mumbai, India.
- **Activators:** Stearic acid with density 0.9–0.9761 g/cm^3 at 15°C and zinc oxide (ZnO) with density 5.55-5.61g/cm^3 at 15°C were supplied by Aldrich Company, Germany.
- **Curing agent:** elemental sulphur as vulcanizing agent with fine pale yellow powder and density 2.04-2.06g/cm^3 at room temperature (25°C ± 1) was supplied by Aldrich Company, Germany.
- **Kaolin:** Egyptian Kaolin used has chemical formula; $Al_2O_3.SiO_2.2H_2O$. Specific gravity 2.6, loss on ignition (L.O.I) 14% max, oil absorption 55(g/100g), and pH 6-7 was from El-Nasr company, Egypt. The chemical composition of kaolin is represented in Table (1).

The other rubber ingredients are the customarily used in rubber industries; solvents and chemicals are of pure grade.

2.1.2. Preparation of doped-kaolin

First, kaolin was doped with small amounts of ammonium molybdate ranging from (0.02-0.1 mol %), the mixture was mixed very well, ground and then calcined in a muffle furnace at 1000ºC; the ramp was set at 20°C/min. The reaction took place according to the following scheme;

$$(NH_4)_2Mo_7O_{24}.4H_2O \xrightarrow{300^oC} MoO_3 + 2NH_4OH + 2H_2O \quad (1)$$

$$7MoO_3 \longrightarrow 7MoO_2 + 1/2O_2 \quad (2)$$

$$2Al_2O_3.4SiO_2.2H_2O + (NH_4)2Mo_7O_{24}.4H_2O \longrightarrow$$

$$2(Al_2O_3)_{1-x}(MoO_2)_x + 4SiO_2 + 2NH_4OH + MoO_2 + 4H_2O \quad (3)$$

According to equation (3), molybdenum oxide which is the result of ammonium moybdate heating in reaction (1) is allocated in the interstitional positions of the Al_2O_3 crystals which is naturally found in kaolin leading to a better-defined crystalline structure of alumina by transferring it from a less-stable phase (γ-Al_2O_3) to a higher stable one (α-Al_2O_3), this behaviour was reported in (Ahmed, 2005) (Yang et al., 2010).

Treated kaolin with the different dopant concentrations will be denoted by symbols to remark them; these symbols are given in Table 2.

2.2. Mixing of rubber samples

Mixing of rubber was carried out on a laboratory two-roll mill (470mm diameter and 300mm working distance). The speed of the slow roll was 24rpm with a gear ratio of 1:1.4. The rubber compounds were vulcanized in an electrically heated hydraulic press at 152±1ºC and 4MPa pressure for optimum cure time (Tc_{90}) (Salmah et al., 2009) as determined for each compound in Table 3.

2.3. Processing of rubber-clay composites

First the uncured rubber was mixed with the essential additives in laboratory as mentioned previously, and then the master-batch containing uncured rubber and additives was mixed with the different loadings of kaolin and

doped-kaolin. After that the composites were sheeted to the required thickness (Yehia et al., 2012), then they were tested according to the following standard methods;

- Rheometric characteristic was determined at 152ºC using a Monsanto Rheometer (model 100) according to ASTM D 2084.
- Tensile tests were determined according to ASTM D 412. Dumb-bell shaped specimens of 2mm thick were cut from the moulded sheets using a Wallace die cutter with crosshead speed of 500cm/min. The tests were performed at 25 ± 3ºC, three specimens were used and the average was calculated in each case.
- ASTM shore A was used to measure hardness of the sample according to ASTM D 2240.
- Swelling was determined according to ASTM D3616.
- The equilibrium swelling Q% was calculated using the following formula;

$$\mathbf{Q_t} = \left\{\frac{(\mathbf{W_s} - \mathbf{W_d})}{\mathbf{W_d}}\right\} \mathbf{X\ 100} \qquad (\mathbf{4})$$

Where W_s is the weight of the swollen sample, and W_d is the weight of the dry sample. The swelling data in toluene for 24 h at 25 ± 1ºC were used to estimate the molecular weight between two crosslinks (M_c), and the crosslink density (ν) was determined by applying the related equations described in Flory-Rehner method as follows (Mohan et al., 2012) (Ahmed and El-Sabbagh, 2011) (Flory, 1943);

$$\boldsymbol{M_C} = \frac{-\boldsymbol{\rho V_S V_r^{1/3}}}{\mathbf{ln(1-}\boldsymbol{V_r}\mathbf{)}} + \boldsymbol{V_r} + \boldsymbol{\mu V_r^2} \qquad (\mathbf{5})$$

Where ρ is the density of rubbers, V_S is the molar volume of toluene (106.35 cm^3 mol^{-1}), μ is the interaction parameter of rubbers; (μ for SBR is 0.446) (Fory, 1943) and V_r is the volume fraction of swollen rubber which can be obtained from the masses and densities of rubber sample and the solvent. The degree of crosslinking (ν) in mole/cc is given by;

$$\mathbf{\nu = 1/M_C} \qquad \mathbf{(6)}$$

2.4. Instrumental analysis

- **X-ray diffraction** was done by Philip′s diffractometer (type PW1390), employing Ni-filtered Cu Kα radiation (λ =1.5404 Å), Japan. The diffraction angle, 2θ, was scanned at a rate of 2°/min. at room temperature.

- **Transmission electron microscopy (TEM)** was done on kaolin and doped-kaolin using (JEOL JX 1230) technique with micro-analyzer electron probe, Japan. This technique can show both the particle shapes and sizes of kaolin and doped-kaolin.

- **Scanning electron microscopy (SEM)** was done using (JEOL JXA- 840A) electron probe micro-analyzer, Japan. For preparing samples, rubber specimen was broken in liquid nitrogen and the cross-section surface was covered with a very thin layer of gold to avoid electrostatic charging during examination.

- **Thermo-gravimetric analysis (TGA)** of the composites was carried out using Perkin Elmer analyzer equipments, USA. The sample weights between 13-45mg were scanned from 50-1000˚C using a nitrogen air flow of 50ml/min and a heating rate of 10˚C/min.

3. Results and discussion

3.1. Characterization of the prepared pigments

Figure 1 representing the XRD charts of kaolin and doped-kaolin showed that the main peaks of kaolin Fig. 1-a are located at d Å 3.341, 3.577, 3.121, 2.812, 4.717, 4.463, 2.566, 2.457, while those of γ-alumina were at 2.129, 1.617, 1.69 as can be seen in Fig. 1-b, whilst the peaks of α-Al_2O_3 formed after doping of kaolin in Figure 1-c appeared at d Å 2.539, 2.486, 2.23, 2.122, 1.977, and 1.816 as very intense and sharp peaks indicating very well crystalline phase. Although the peaks indicating the change in alumina phase were intense, the main peak of kaolin at d Å 3.341 was detected in the three charts indicating that the change in alumina phase occurred without affecting the main peak of kaolin, i.e. its chemical structure is the same.

Figures 2 and 3 show the morphology of kaolin and the different doped-kaolin using SEM and TEM, from the featured photos it can be seen that kaolin has huge hexagonal platelet particles. Doped-kaolin appeared as ordered huge size plates when the dopant concentration was low in K1 Figure 2b, while it possesses a smaller, more compact and ordered platelets as the dopant concentration increases in K5 Figure 2c.

These shapes were confirmed in TEM photos shown in Figure 3, which showed that kaolin plates were homogenous hexagonal plates. In case of doped-kaolin, samples containing high dopant concentration (K5) showed more homogenous and geometrically defined plates than in case of kaolin containing lower dopant concentration (K1). These plate structures of clay help in slippage of rubber chains from the surface of clay particles leading to improved elasticity, this elasticity is attributed to the plasticizing and the conformational effects on the polymer at the clay-matrix interface indicating that the clay particles are in stacked condition and polymer chains are diffused inside the clay itself (Ahmed et al., 2011).

3.1. Rheological properties

The processability of SBR/kaolin composites was determined by evaluating the rheometric characteristics. From the cure characteristics of the composites, it can be observed that the minimum torque $\mathbf{M_L}$ which is a measure of the viscosity and filler-filler inter-aggregations of the composites, increases with the loading of filler and then decreases as can be seen in Figure 4a. From the figure it can be detected that, M_L values are in direct relationship with filler loadings. Maximum torque $\mathbf{M_H}$ which is an indication of the shear modulus of the vulcanizates, increased with increasing the kaolin loading having the different concentrations of dopant (K1-K5). The increase in M_H was attributed to the presence of doped-kaolin particles in the matrix which reduces the mobility of the molecules due to its hard particles and consequently increases the torque of the vulcanizates (Lui, 2008). Also from Figure 4 and Table 3, the data obtained showed that the addition of kaolin or doped-kaolin to SBR rendered the scorch time t_{s2} at the same level as that of unfilled SBR, while cure time t_{c90} decreases for initial filler loading (10phr) and then there was an increase as the loadings increase. The reason for lower cure time values in case of SBR containing 10phr of doped-kaolin was due to the increase in SBR thermal transition which promotes the vulcanization process, also the doping of kaolin leads to increased specific surface area which results in improving the filler-filler and filler-matrix interactions (Marzocca, 2007) (Wu and Tien, 2013). On the other hand, the value of cure rate index (CRI) which is a direct measure of the fast curing nature of rubber composites for SBR/K1-K5 composites are higher than that of unfilled SBR which can be declared by the presence of doped-kaolin that acts as an effective vulcanizing agent.

The changes in rheometric torque with filler loading can be used to characterize the filler-matrix interaction or reinforcement, this can be represented by the reinforcement factor α_f which is calculated from the rheographs (Mousa, 2013) (Wu and Tian, 2013) and given by;

$$\boldsymbol{\alpha_f = \frac{\Delta M_{max(filler)} - \Delta M_{max(gum)}}{\Delta M_{max(gum)}}} \qquad (7)$$

Where ΔM_{max} is the maximum changes in torque during vulcanization, α_f is a factor representing the reinforcement factor or the rubber-filler interaction and it is independent on the cure system and closely related to the filler morphology. Also, α_f can be calculated from the changes in torque that occur during vulcanization of the loaded and unloaded composites. The benefit of Eqn. 7 lies not only on the fact that it defines the filler specific constant determined by the filler structure but also in defining the degree of crosslinking density of the filler (Wolff and Wang, 1992). Table 3 represents the calculated α_f, and it can be clearly seen that in case of SBR containing kaolin (K) and doped-kaolin (samples containing K4 and K5), the value of α_f is decreased with filler loading. Also, it can be noticed that the values of α_f in case of SBR loaded with K1-K3 are not regular; this may be due to agglomeration of filler in the matrix (Ward et al., 2013) which clearly reveals that K4 and K5 are well dispersed in SBR matrix.

3.2. Mechanical properties

SBR ultimate properties are not only affected by doped-kaolin, but also a marked increase in the stiffness was detected as well for SBR/ (K1-K5) composites. Fig. 5 depicts the stress-strain curves of the composites, and it can be seen that for a given strain all filled systems exhibited higher stresses than the unfilled. Although the vulcanizates were loaded with kaolin doped with different concentrations of ammonium molybdate there is small difference between the different SBR composites (SBR/K1-K5) showing all the curves to follow a similar pattern; initially a very rapid stress growth takes place even with low dopant concentration (SBR/K1-K3) which reflects the existence of strong matrix-filler bonds that restrict the deformation ability of the composite (Lui et al., 2008), then comparatively higher value of failure stress was obtained for 20phr of SBR/K5 composite followed by 20phr of SBR/K4.

Mechanical properties are strongly dependent on the dispersion of filler particles in the rubber matrix. Figure 6a shows the effect of doped-kaolin on the tensile strength of SBR composites, which revealed that the

tensile strength was improved significantly with increasing filler content up to 30phr. Increasing doped-kaolin beyond 50phr led to a slight decrease in the tensile strength as in (SBR/K1, K2 & K3) composites. Any further increase in dopant leads to an increase in the tensile strength with the increase of ammonium molybdate (dopant) content in kaolin up to a maximum value 6.75MPa for SBR/K5, while less concentration of ammonium molybdate was accompanied by a decrease in tensile strength values as in (SBR/K4). This phenomena can be attributed to that the conversion of γ-alumina to α-alumina takes place gradually, i.e. at first entering the dopant introduced to alumina crystals in low concentrations leads to small distortion, then by the gradual increase of the dopant concentration its particles begin to allocate themselves tidely in the interstitional positions between the crystal edges. Further increase in dopant concentrations, led to the scatter of the dopant particles in the crystals leading to the appearance of new distortion, and this is the reason that SBR containing K4 exhibited better properties than SBR containing K5 (Ahmed, 2005) (Yang et al., 2010).

Figure 7 showed that hardness and modulus at 100% strain were increased after the addition of kaolin and doped-kaolin, and this increase is in direct relation with the loadings of doped-kaolin, while in contrast their elongation at break displayed in Figure 7b showed an opposite trend. This decrease in the elongation at break is attributed to the increase of micro-defect, caused by stronger filler-filler interaction than filler-rubber interaction with doped-kaolin. Hardness and modulus at 100% strain were increased because introduction of doped-kaolin into rubber matrix led to an increase in the crosslinking between polymer molecules reducing their mobility, and thus increasing the modulus and strength and at the same time improving the hardness and other mechanical parameters (Wolff, 1996). It was also found that, high hardness and modulus are due to the high crosslink density at SBR/K4.

3.3. Swelling properties

Figure 8a represents the effect of kaolin and doped-kaolin loadings on swelling percentage of SBR composites. It was observed that rubber composites containing 0.06 or 0.08 mol% of ammonium molybdate as dopant (K3 & K4) gave better resistance toward penetration of toluene solvent compared to other samples. As discussed earlier, this is due to the better interaction between doped-kaolin and styrene-butadiene rubber compared to SBR/kaolin composites. Recent researches reported that, as crosslink density increases the molecular movement of the rubber is reduced and makes it more difficult for toluene to penetrate through the rubber (Balachandran et al., 2012). The obtained values of crosslink density are also plotted in Figure 8b, these values indicated that doped-kaolin content increased the apparent crosslink density (Balachandran et al., 2012) which reflected decrease in the equilibrium swelling of SBR/(K1-K4) as compared to SBR/kaolin and also SBR/K5 composites. This may be attributed to the formation of more crosslinks in the vicinity of kaolin owing to the chain segments facilitating the crosslink formation, and consequently an increase in the rubber-filler interaction will be constructed on the expense of filler-filler interaction (El-Sabbagh et al., 2006) (Ahmede et al., 2013). These results are in good agreement with the results of the mechanical properties which indicated that K4 containing 0.08mol % ammonium molybdate as a dopant is the optimum concentration of the doped-kaolin, (i.e. best concentration of dopant in kaolin) that exhibited the best properties among the group.

3.4. Effect of thermal oxidative aging on the mechanical properties

The vulcanized samples were heated in an air oven at 90°C up to 7 days, and then the mechanical properties were re-measured and plotted graphically in Figure 9a-c. From these figures it can be seen that, the retained values of the measured properties initially increased due to further corsslinking formed during aging that counteracted the degradation process in the initial time. On the other hand, these values decreased with increasing aging time due to some sort of degradation. SBR composites containing K1, K4 and K5 exhibited the highest efficiency with aging and the relationship between these plotted parameters in Figure 9a-c can be expressed by equation 8;

$$Y = Ae^{BX} \qquad (8)$$

Where Y represents either the tensile strength or the strain at break, X is the aging time and B is the slope of the line. The first derivative of this equation dY/dX is the gradient of the curve which can give the rate of change in the property; and this is expressed by equation 9.

$$\frac{dY}{dX} = ABe^{BX} \qquad (9)$$

Consequently, the minimum slope means maximum rate of change in the composite properties which defines the efficiency of SBR/doped-kaolin. The addition of K1-K3 to SBR reduced the extent of aging heat by lowering the percentage change in tensile properties and elongation at break. It is also noticed that, the increase of filler concentration in SBR loaded with K4 and K5 increased the retained values of the different properties.

Therefore, the use of doped-kaolin in higher concentration improved thermal heat resistance as in Figure 9b. Kaolin layers may act as barriers for the diffusion of degradation products entering into the interior of the rubber product, however the loss in elongation at break after aging found in Figure 9c may be due to the increase in crosslinking density upon aging which lead to restriction of chain extension and decrease the chain length between crosslinking points. Stress at 100% strain Figure 9a was found to be well correlated with the aging time of SBR composites with/without doped-kaolin in accordance with the power equation 10;

$$\mathbf{Y = ABX^{(b-1)}} \qquad \mathbf{(10)}$$

Where Y represents the stress at 100% strain and X is the aging time of SBR compounds, while dY/dX gives the change in the rate of the property. Equation 11 illustrated the efficiency of doped-kaolin which affected positively the mechanical properties of the composites.

$$\mathbf{\frac{dy}{dx} = ABX^{(b-1)}} \qquad \mathbf{(11)}$$

3.5. Thermal gravimetric analysis

One of the most well accepted methods for studying the thermal properties of polymeric materials is the thermo-gravimetric analysis. Thermo-gravimetric curves (TGA) provided information about thermal stability and extent of the polymeric material degradation. The heating process showed a lot of changes in the material and finally leaving behind the inorganic fillers as residue (El-Sabbagh and Ahmed, 2015). Table 4 showed that rubber composites filled with 30phr of doped-kaolin exhibited more heat resistance and thermal stability compared to unfilled SBR.

From Figure 10 a, b it was clear that thermal degradation occurred in two stages. First, initial thermal degradation temperature (T_i) representing the peak onset temperature of degradation, and (T_f) which is the final decomposition temperature. In these temperature regions, mass loss was due to the thermally activated depolymerization mechanism of SBR into cyclic oligomeric species which are formed by an intramolecular re-arrangement reaction mechanism that can continue along the SBR chain until the chain is too short or the small molecules are carried away by the gas stream (Ismail et al., 2004). All studied samples exhibited an initial small mass loss attributed to the elimination of volatile components such as water, and ammonia residue (Ahmed et al., 2011).

SBR showed T_i value of 337˚C, this temperature increased in case of SBR containing doped-kaolin with increasing the ammonium molybdate (dopant) content up to a maximum value at 360˚C for SBR/K4 composites. Any further increase in concentration of ammonium molybdate content was accompanied by decrease in the Ti values. Also, T_f for SBR/K4 was higher than that of the other concentrations of SBR/doped-kaolin as can be seen in Table (4). T_f was found between 625˚C-950°C for SBR/doped-kaolin composites, while 50phr of SBR/doped-kaolin gave the highest residual weight percentage indicating that these composites were more stable than unfilled SBR which declared the fact that addition of doped-kaolin to SBR offered composites with higher thermal stability.

The above described results are summarized in Table 4, which cleared that the matrix degradation temperature and the increase in the corresponding onset with the addition of kaolin to SBR are represented. On the other hand, the height of the peak at any temperature gave the rate of mass change, i.e. the rate of degradation at this temperature. Also, some endothermic peaks were observed in differential thermo-gravimetric (DTA) curve indicating that the vulcanization of rubber or SBR/doped-kaolin was incompletely curved. There was shift in endothermic peak after adding doped-kaolin to rubber, i.e. the thermal degradation peak temperatures of these rubber composites are shifted to higher temperature. The better thermal stability was attributed to the barrier effect of the finely dispersed particles which hindered the diffusion of small molecules generated during the thermal decomposition (Abdul Kader and Bhowmick, 2003) (Amraee et al., 1995). The decrease in thermal stability at higher concentration of SBR/K5 at 50phr was due to the lowering of the crosslink density so that the required energy for thermal degradation exhibited lower extent.

3.6. Phase Morphology

The morphology of the composites and the dispersion degree of kaolin and doped-kaolin in SBR matrix were studied using SEM technique, the photos are shown in Figure 11. The micrograph of unfilled SBR (at 1000x) shown in Figure 11a revealed the good distribution of rubber ingredients (such as zinc oxide and sulphur curatives) in SBR matrix. On the other hand, SEM micrographs of SBR/kaolin composites loaded with 50phr shown in Figure 11b, c &d revealed the presence of large aggregates with non-uniform dispersion which is attributed to the poor adhesion between kaolin and SBR, while it can be deduced that domain size decreased in SBR/K3 and SBR/K4. From Figure 11e &f the micrograph showed that doped-kaolin is dispersed uniformly in SBR matrix and its domain

size was remarkably decreased. This good dispersion is attributed to the strong adhesion between K3 and K4 with SBR; and may be also due to that α-alumina has a very stable phase which is hardly affected by the surrounding medium (Camino et al., 2002) (De-Oliveira et al., 2006) (Calderon et al., 2008). At contrast, in case of SBR/K5 represented in Figure 11g it can be noticed that at this concentration doped-kaolin have weak interfacial interaction with rubber because the filler dispersion is not uniform, this poor filler dispersion reduced the filler-rubber interaction and consequently reduced the physical properties which may be the reason that the tensile strength was decreased at this concentration (Golbeiewski and Galeski, 2007).

Table 1. Chemical composition of kaolin

Component	**wt.%**
Al_2O_3	31.5
SiO_2	50.5
Fe_2O_3	1.87
TiO_2	2.26
MnO	0.01
P_2O_5	0.08
Na_2O	0.1
CaO	0.66
MgO	0.9
K_2O	0.07

Table 2. Symbols of doped-kaolin

Dopant concentration (mol %)	**Symbol**
0.02	K1
0.04	K2
0.06	K3
0.08	K4
0.1	K5

Table 3. Formulations and rheological characteristics of styrene-butadiene rubber loaded with kaolin and doped-kaolin (K1- K5) composites at (152 ± 273ºC)

Filler loading, phr	**-**	**10**	**20**	**30**	**40**	**50**
Kaolin	**Rheometric characteristic of SBR/kaolin (K)**					
T_{s2}, min	6	6.75	7	7.5	6.75	6.38
α_F	-	4.4	2.5	2.03	1.6	1.6
0.02 mol% of dopant in kaolin (K1)	**Rheometric characteristics of SBR/K1**					
T_{s2}, min	6	6.75	7	6.5	6	6.5
α_F	-	4.4	3.25	1.067	1.48	1.56
0.04 mol% of dopant in kaolin (K2)	**Rheometric characteristics of SBR/K2**					
T_{s2}, min	6	6.125	5.5	6.25	6.375	5.625
α_F	-	3.6	1.5	1.733	1.6	1.52
0.06 mol% of dopant in kaolin (K3)	**Rheometric characteristics of SBR/K3**					
T_{s2}, min	6	5.25	5.25	4.75	4.75	5
α_F	-	0.8	1.2	1.53	1.6	1.92
0.08 mol% of dopant in kaolin (K4)	**Rheometric characteristics of SBR/K4**					
T_{s2}, min	6	5.25	6.5	5.875	5.75	6
α_F	-	- 3.4	3.35	3.2	2.425	2.02
0.1 mol% of dopant in kaolin (K5)	**Rheometric characteristics of SBR/K5**					
T_{s2}, min	6	7	6.625	5.25	5.75	5.5
α_F	-	4.3	3.6	2.77	2.525	2.04

Notes: Base recipe in phr (part per hundred parts of rubber): SBR 100; stearic acid 2; zinc oxide 5; CBS (N-cyclohexyl-2-benzothiazole sulfenamide) 0.8; IPPD (N-isopropyl, N`phenyl-p-paraphenylene diamine); sulphur 2.

t_{s2} is scorch time; α_F is specific constant for reinforcement of fillers (i.e. activity of filler).

Table 4. Thermo-gravimetric data for Styrene butadiene rubber (SBR) and its composites with 50phr of kaolin and different concentrations of doped-kaolin

Sample identification	T_i (˚C)	T_f (˚C)	Residual, (%)	Peak temp. (T_{max}, ˚C)	Peak height (%/min.)	Area, %
SBR	337	628	5.25	387	-5.75	-54
SBR/kaolin (K)	354	608	33	411	-8.9	-35.34
SBR/K1	347	675	36.26	421	-7.75	- 31.9
SBR/K2	354	700	35.69	425	-5	-19.6
SBR/K3	341	785	35.5	410	-6	-23.6
SBR/K4	360	950	34	426	-4	-17.4
SBR/K5	323	625	34.3	411	-8	-33.8

T_i - initial thermal decomposition temperature, T_f - final thermal decomposition temperature

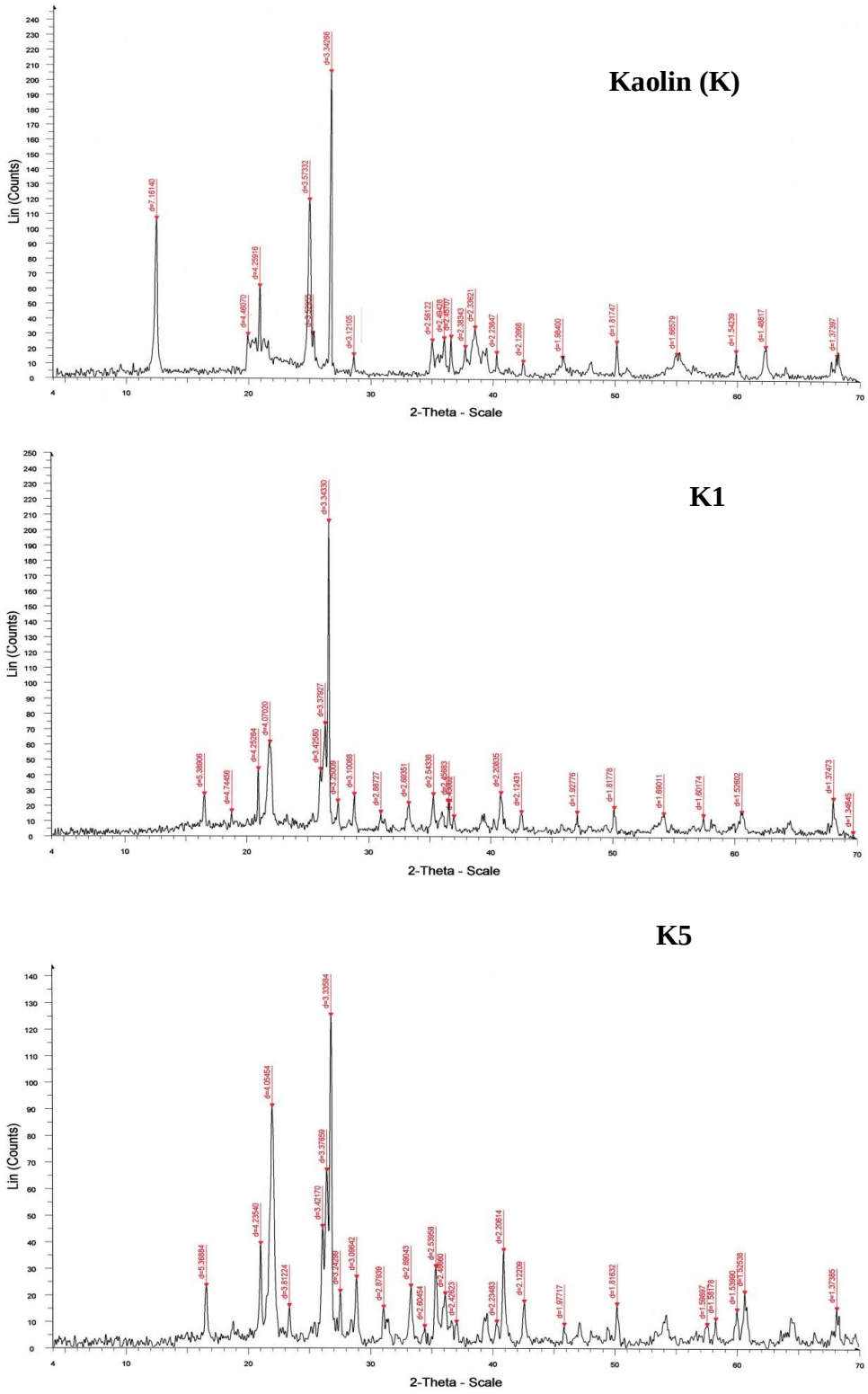

Figure 1. XRD charts of (a) kaolin, (b) K1 and (c) K5

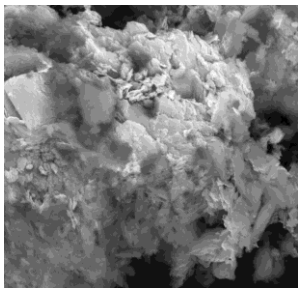

(a)

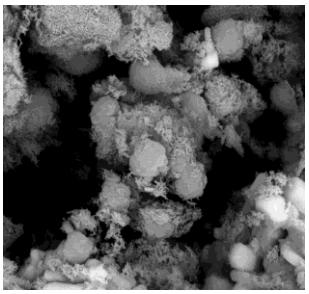

(b) K1

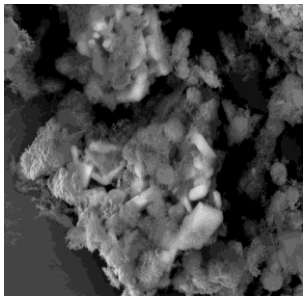

(c) K5

Figure 2. SEM micrographs of (a) kaolin (K), (b) K1 and (c) K5 at magnification 150X

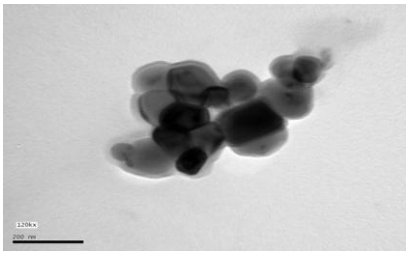

(a) Kaolin

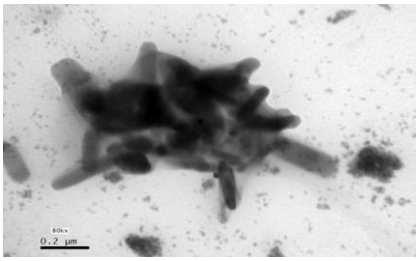

(b)

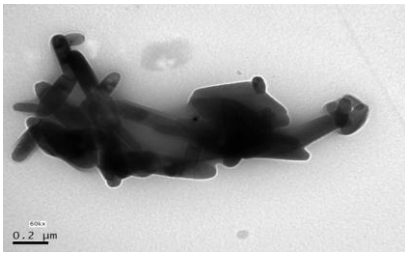

(c)

Figure 3. TEM micrographs of (a) Kaolin (K), (b) K1 and (c) K5 at

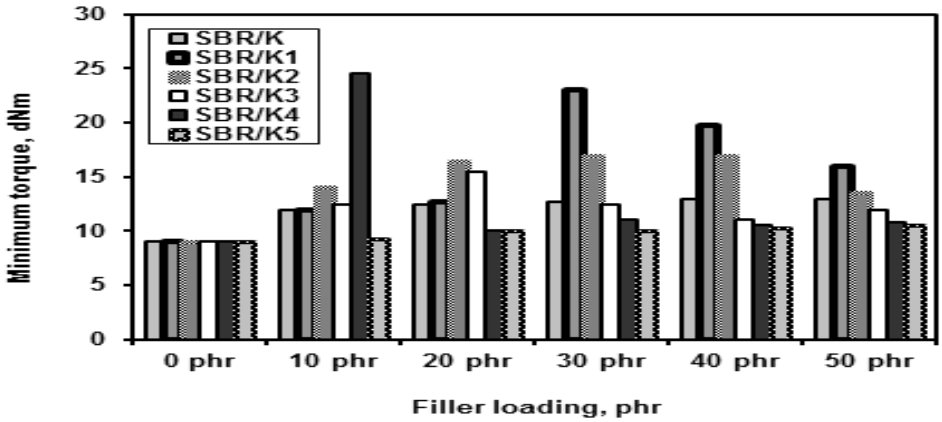
SBR/K
SBR/K1
SBR/K2
SBR/K3
SBR/K4
SBR/K5
Minimum torque, dNm
0
5
10
15
20
25
30
0 phr
10 phr
20 phr
30 phr
40 phr
50 phr
Filler loading, phr

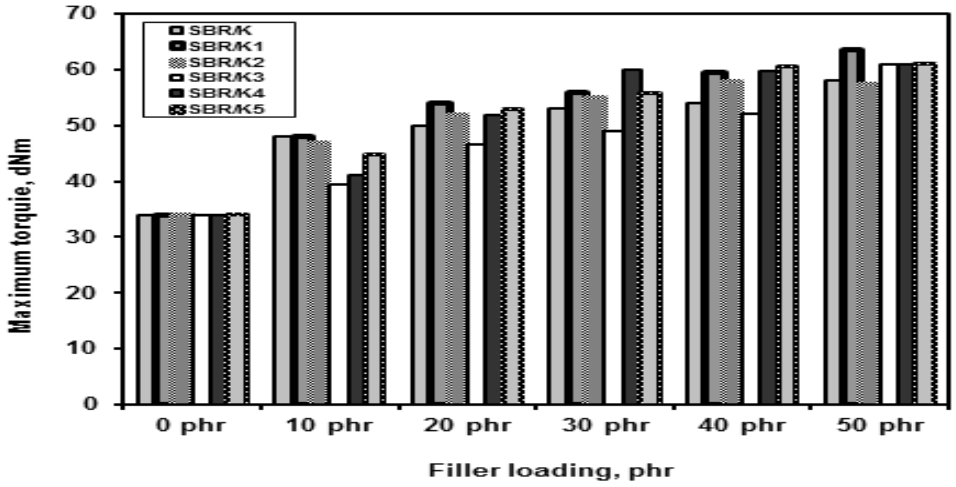
SBRK
SBRK1
SBRK2
SBRK3
SBRK4
SBRK5
Maximum torquie, dNm
0
10
20
30
40
50
60
70
0 phr
10 phr
20 phr
30 phr
40 phr
50 phr
Filler loading, phr

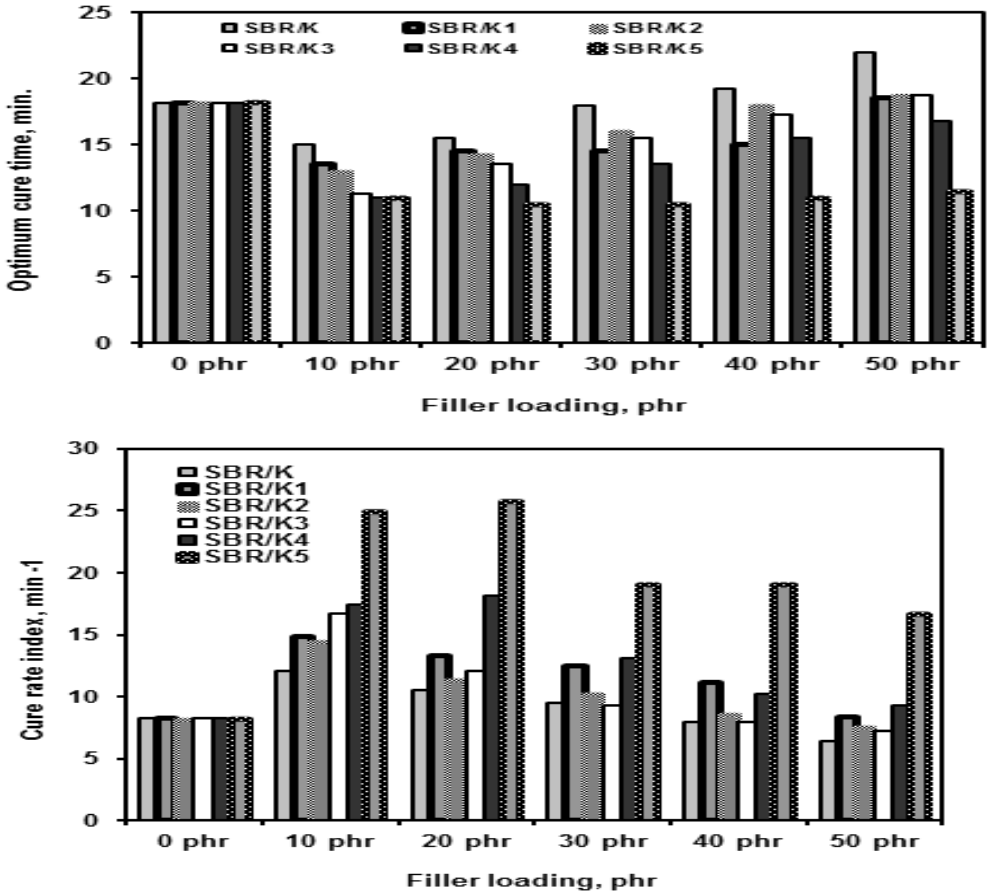

Figure 4. Variation of (a) minimum torque, (b) maximum torque, (c) optimum cure time, and (d) cure rate index versus filler loading of kaolin and doped-kaolin

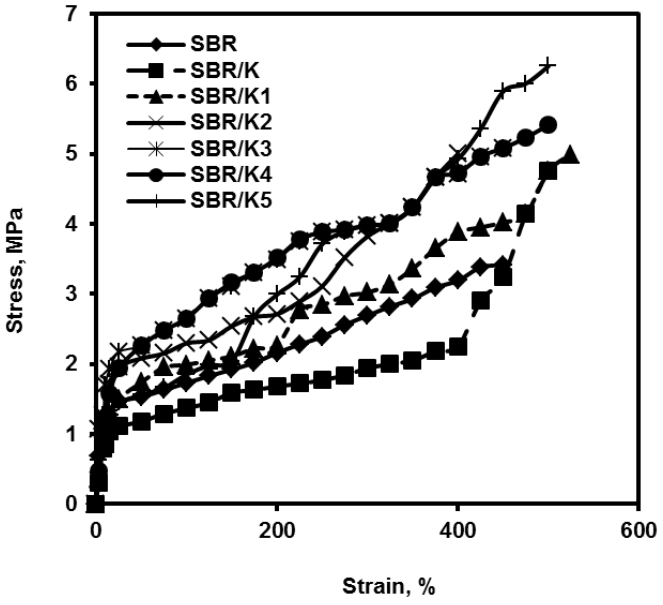

Figure 5. Stress-strain curves of SBR loaded with 20phr of kaolin and doped-kaolin

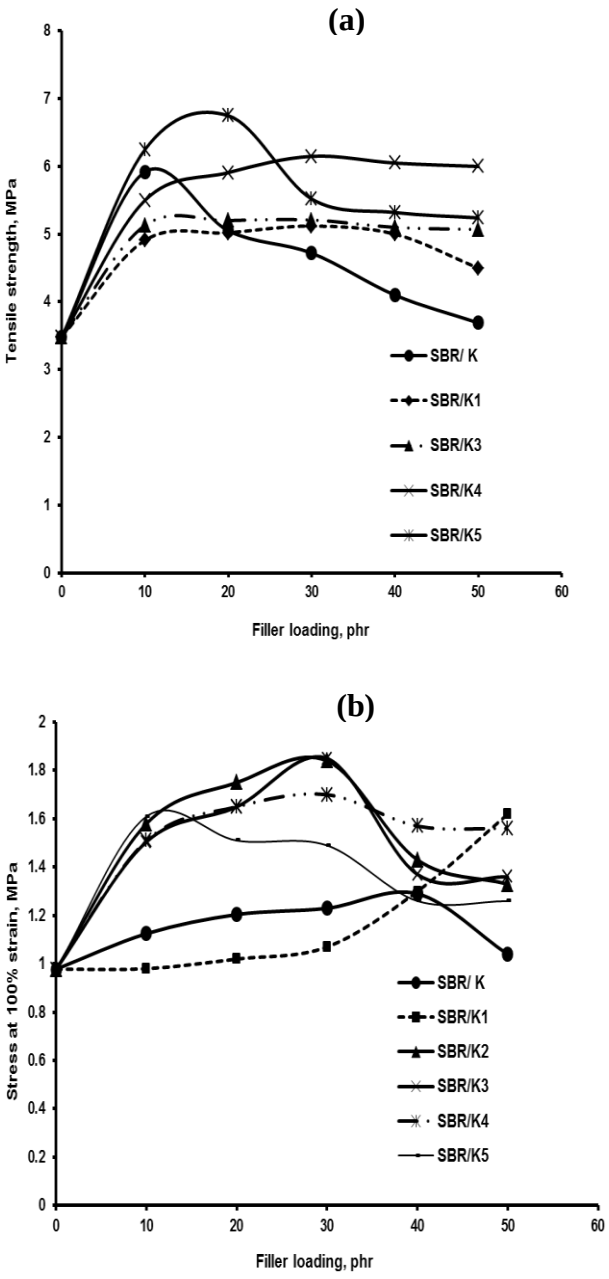

Figure 6. The relation between (a) tensile strength and (b) stress at 100% strain versus SBR loading with 30phr of kaolin (K) and doped-kaolin (K1-K5)

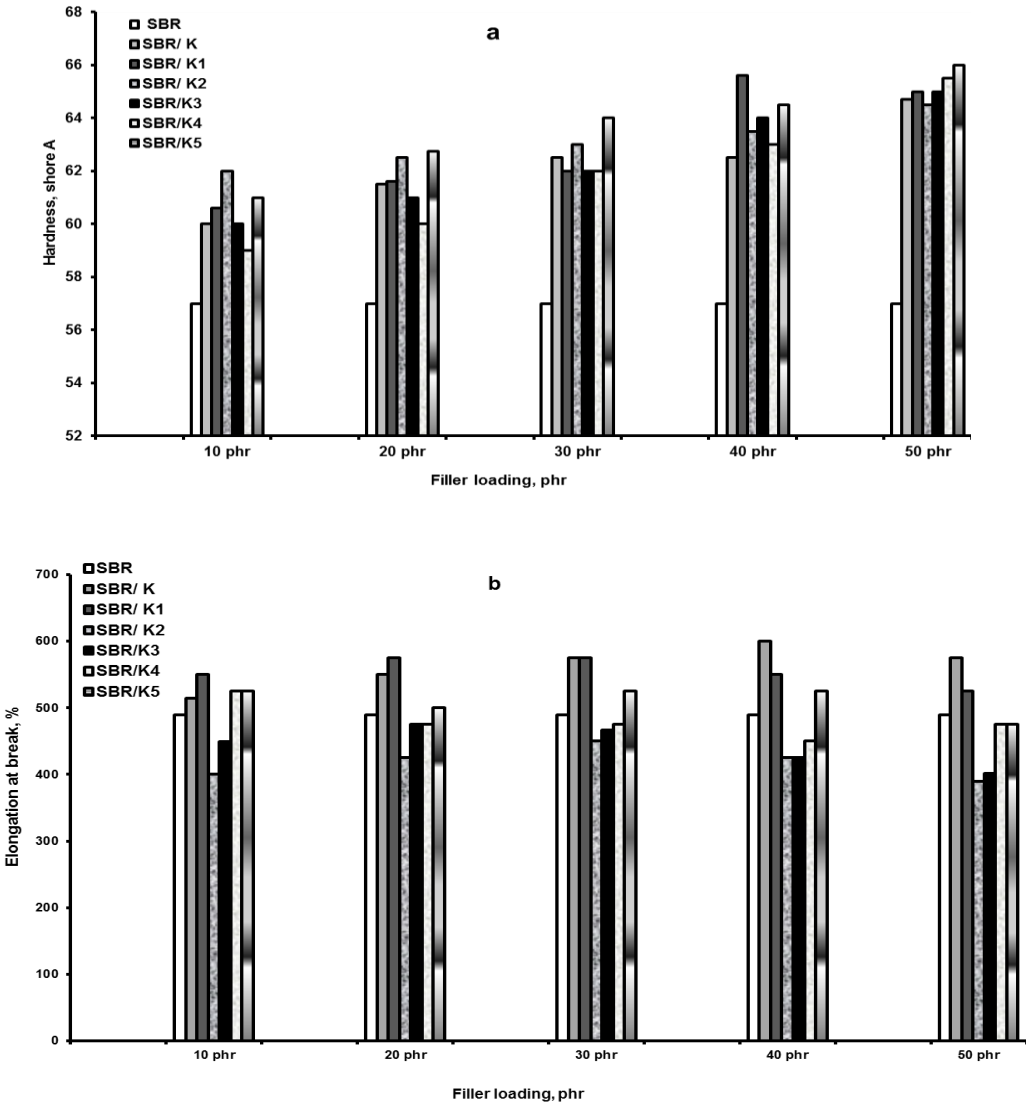

Figure 7. The relation between (a) hardness and (b) elongation at break versus SBR loading with 30phr of kaolin (K) and doped-kaolin (K1-K5)

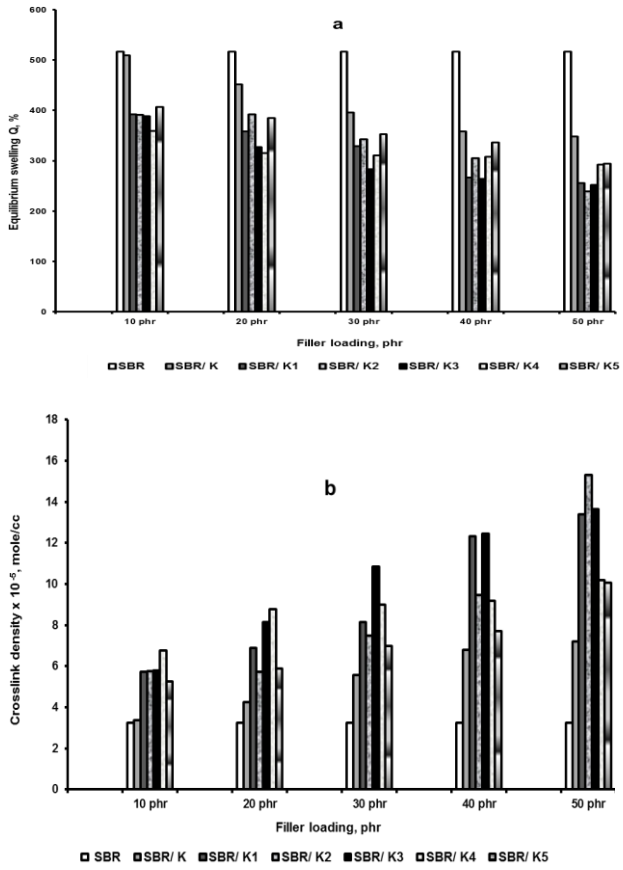

Figure 8. Variation of (a) equilibrium swelling and (b) crosslink density versus SBR loading with kaolin (K) and doped-kaolin (K1-K5)

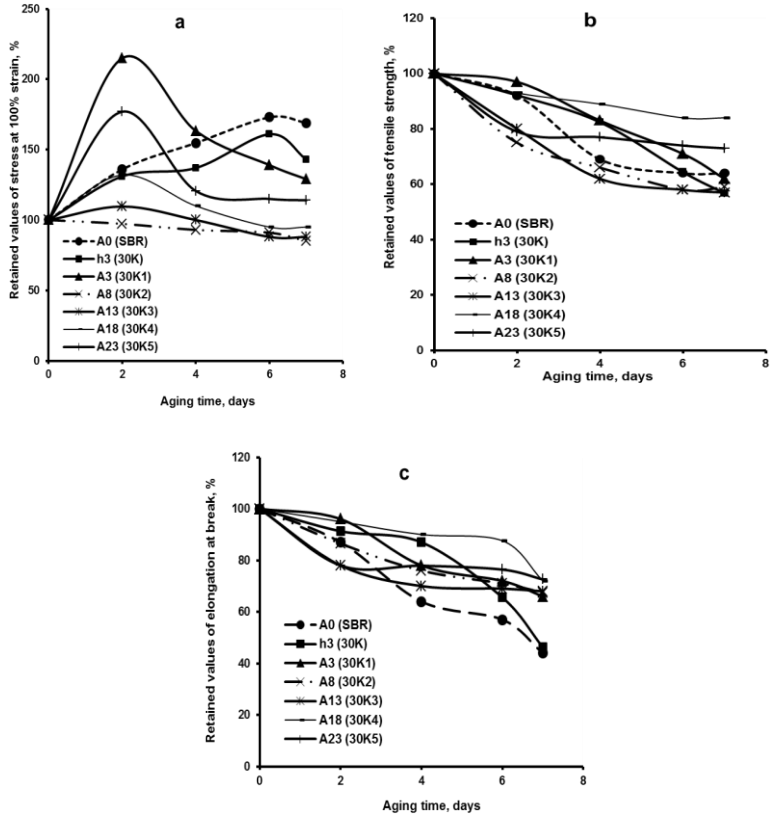

Figure 9.The relation between retained values of (a) stress at 100% strain, (b) tensile strength, and (c) elongation at break versus aging time

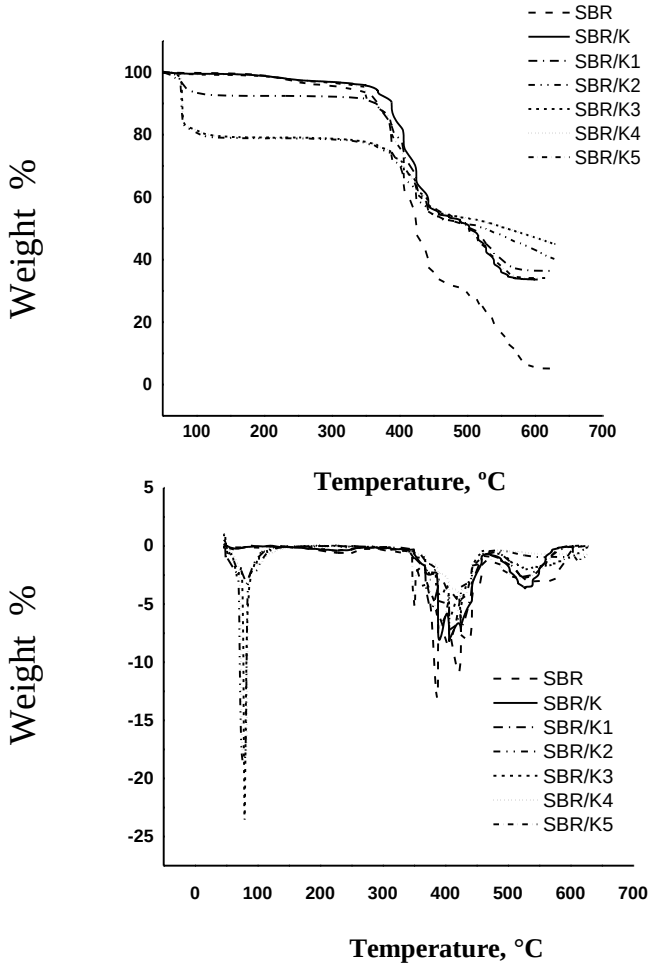

Fig.10. TGA curves of (a) weight loss %, (b) derivative weight % of SBR loaded with 30phr kaolin and doped-kaolin

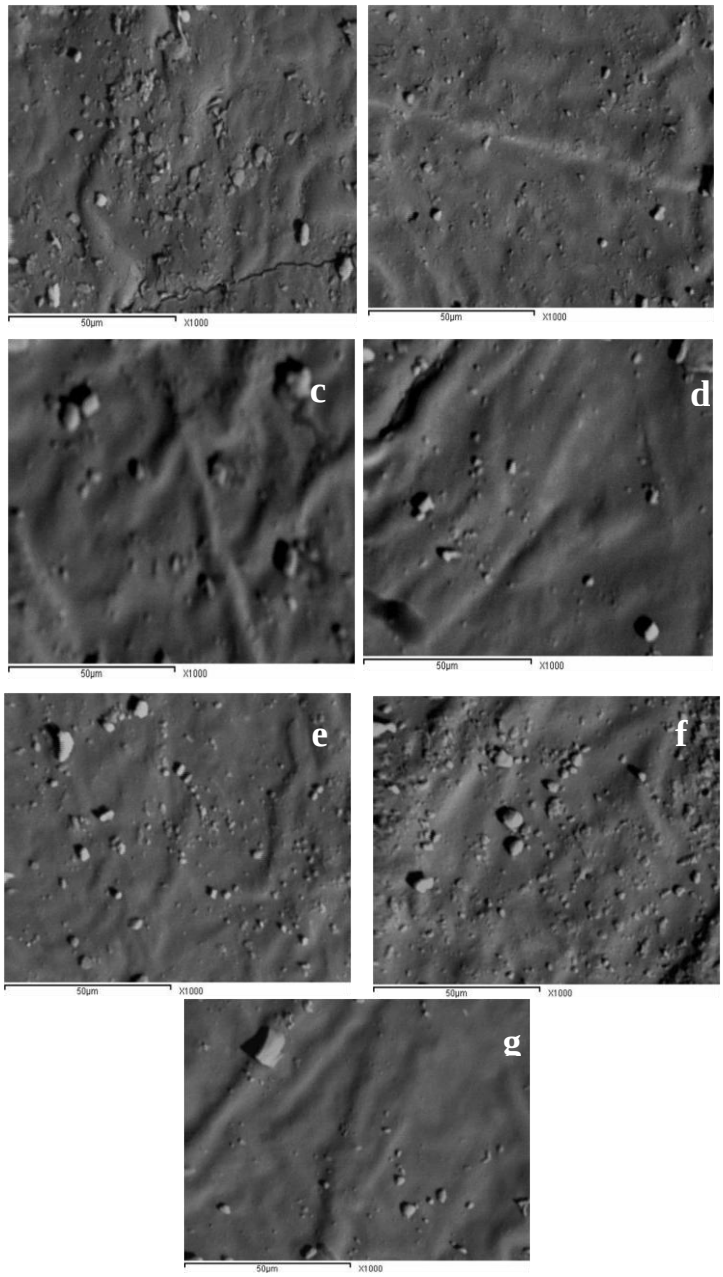

Figure 11. SEM micrographs of (a) SBR and SBR loaded with 50phr of (b) SBR/K, (c) SBR/K1, (d) SBR/K2, (e) SBR/K3, (f) SBR/K4 and (g) SBR/K5 at magnification X10^3

Conclusions

In the present work kaolin was doped with small amounts of ammonium molybdate ranging from 0.02-0.1 mol%. Kaolin and doped-kaolin were added to styrene-butadiene rubber (SBR) in different concentrations. According to the previous data, it can be concluded that;

1. The rheological properties of SBR/doped-kaolin composites are higher than those of SBR/kaolin or unfilled SBR; this can be declared by that doped-kaolin act as an effective vulcanizing agent.
2. Adding an appreciable quantity of doped-kaolin can help the rubber vulcanizates to tolerate thermal oxidative aging. On the other hand, incorporation of doped-kaolin into SBR rubber also improved the physico-mechanical properties; these properties became better than unfilled SBR vulcanizates after heat resistance testing.

3. Swelling behaviour of SBR containing doped-kaolin was better than that of SBR containing kaolin; this is due to the smaller particles of doped-kaolin that prohibited toluene penetration to the matrix. Also, it is due to the better interaction of doped-kaolin with rubber compared to that of kaolin.

4. Thermal studies showed that doped-kaolin was the best in its thermal stability leaving the highest residue.

5. Additions of doped-kaolin to SBR improved the tensile and hardness, the optimum properties were those exhibited by SBR/K4 composites containing kaolin doped with 0.08 mol% ammonium molybdate. This enhancement in properties was attributed to strong interface interaction between the rubber matrix and the filler.

References

Abdul Kader, M., Bhowmick, A.K. (2003): Thermal ageing degradation and swelling of acrylate rubber fluoro rubber and their blends containing poly-functional acrylates. J. Polym. Degrad. & Stability, 79: 283-295.

Ahmed, N.M. (2013): Comparative study on the role of kaolin, calcined kaolin and chemically treated kaolin in alkyd-based paints protection of steel. J. Pigm. & Res. Technol, 42 (1): 3-14.

Ahmed, N.M. (2005): A new approach to enhance the anticorrosive properties of treated Egyptian kaolin. J. Anticorrosion Methods and Materials, 52 (3): 167-175.

Ahmed, N.M., El-Nashar, D.E., El-Messieh, S.L. (2011): Utilization of new micronized and nano-CoO.MgO/kaolin mixed pigments in improving the properties of styrene-butadiene rubber composites, Materials & Design 32: 170-182.

Ahmed, N.M., El-Sabbagh, S.H. (2011): The influence of hybrid phosphate-alumina pigments on properties of Ethylene propylene diene rubber composites. J. Mater. & Des. 32: 303-321.

Ahmed, N.M., Tawfik, M.E., Ward, A.A. (2013): Characterization of a Polymer Composite from Treated Kaolin and Unsaturated Polyester Based on PET Waste. J. Polym. & Composites, 34: 1223-1234.

Amraee, I.A., Katbab, A.A., Aghafarajollah, S.H. (1995): Qualitative and Quantitative Analysis of SBR /BR blends by thermogravimetric analysis. J. Rubb. Chem. & Technology 69: 130-136.

Balachandran, N.A.; Kurian, P.; Joseph, R. (2012): Effect of aluminium hydroxide chlorinated polyethylene, decabromo biphenyl oxide and expanded graphite on thermal, mechanical and sorption properties of oil-extended ethylene-propylene-diene-terpolymer rubber. J. Mater. & Des., 40: 80-89.

Calderon, J.U., Lennox, B., Kamal, M.R. (2008): Thermally stable phosphonium-montmorillonite organoclays. J. Appl. Clay Sci., 40: 90-98.

Camino, G., Lomakin, S.M., Lageard, M. (2002): Poly-dimethylsiloxane thermal degradation, part 2. The degradation mechanisms. Polymer, 43: 2011-2015.

Conceicao, S.I., Velho, J.L., Ferreira, J.M.F. (2003): Influence of de-agglomeration and carboxymethyl cellulose binders on rheological behaviour of kaolin suspensions. J. Appl. clay Sci., 23: 257-264.

De-Oliveira, L.C.S., DE-Arruda, E.J., Da-Costa, R.B., Goncalves, P.S., Job, A.E.(2006): Evaluation of Thermal Behaviour of Latex Membranes from Genetically Improved Rubber Tree (Hevea Brasiliensis). Thermochimica Acta, 445: 27-31.

El-Sabbagh, S.H., Ahmed, N.M. (2015): Enhancement of styrene-butadiene rubber composites using kaolin covered with metal oxide pigments. Pigment & Resin Technology, 44: 57-73.

El-Sabbagh, S.H., Ahmed, N.M., Selim, M.M. (2006): Preparation and characterization of high performance rubber vulcanizates loaded with modified aluminium oxide. J. Pigm. & Res. Technology, 35: 119-131.

Flory, J., Rehner, J. (1943): Statistical mechanics of cross-linked polymer network, I: rubber like elasticity. J. Chem. & Phys., 11: 512–520.

Golebiewski, J., Galeski, A. (2007): Thermally stability of nanoclay polypropylene composites by simultaneous DSC and TGA. J. Composites Sci. & Technology. 67: 3442-3447.

Hernandez P.C., Hernandez L., Flores-Velez, L.M., Del Castillo, L.F., Dominguez, O. (2007): Processing and Mechanical Properties of Natural Rubber-$ZnFe_2O_4$ Nanocomposites. JMEPEG, 16: 470-476.

Ismail, H., Osman, H., Ariffin, A. (2004): A comparative study on curing characteristics, mechanical properties, swelling behaviour, thermal stability, and morphology of feldspar and silica in SMRl vulcanizates. J. Polym. & Plast. Technol. Eng., 43: 1323-1344.

Johns, R.E., Berube, R.R., Slepetys, R.A. (1990): Chemically structured kaolin: a new coating pigment. Tappi Journal, 73: 77-84.

Lui, Q., Zhang, Y., Xu, H. (2008): Properties of vulcanized rubber nano-composites filled with nano-kaolin and precipitated silica. Applied Clay Science, 42: 282-287.

Markovic, G., Samarzija-Jovanov, S. (2010): Thermal stability of CR/CSM rubber blends filled with nano- and micro-silica particles. J. Therm. Anal. Calorimetry, 100: 881-888.

Marzocca, A.J. (2007): Evaluation of the polymer-solvent interaction parameter μ for the system cured styrene butadiene rubber & toluene. J. European Polymers 43: 2682-2689.

Mohan, T.P., Kuriakose, J., Kanny, K. (2012): Water uptake and mechanical properties of natural rubber-styrene butadiene rubber (NR-SR) Nanoclay composites. J. Ind. Eng. Chem., 18: 979-985.

Mousa, A. (2013): The effect of feldspar and kaolin on mechanical performance of SBR/LDPE composites. International Journal of Industrial Chemistry, 4: 26.

Panda, A.K., Mishr, B.G., Mishra, D.K., Singh, R.K. (2010): Effect of sulphuric acid treatment on the physic-chemical characteristics of kaolin clay. Colloids and Surfaces A: Physicochemical and Engineering Aspects, 363: 98-104.

Salmah, H., Ruzaidi, J.C.M., Supri, A.G. (2009): Compatibilisation of Polypropylene/Ethylene Propylene Diene Terpolymer/Kaolin Composites: The Effect of Maleic Anhydride- Grafted Polypropylene. J. Phys. Sci., 20: 99-107.

Ward, A.A., El-Sabbagh, S.H., Abd El-Gaffar, M.A. (2013): The Dielectric and Physical Properties of Phosphate Pigment Rubber Composites. KGK, Kautschuk Gummi Kunststoff 6: 29-40.

Wolff, S. (1996): Chemical Aspects of Rubber Reinforcement by Fillers. J. Rubber Chem. & Technology, 69: 325-338.

Wolff, S., Wang, M.J. (1992): Filler Elastomer Interactions. Part IV. The Effect of the Surface Energies of Fillers on Elastomer Reinforcement. J. Rubber Chem. & Technology 65: 329-342.

Wu, W., Tian, L. (2013): Formulation and morphology of kaolin-filled rubber composites. Applied Clay Science, 80: 91-97.

Wu, W., Tien, L. (2013): Formulation and morphology of kaolin-filled rubber composites. J. Appl. Clay Sci., 80-81: 93-97.

Yang, H., Liu, M., Ouyang, J. (2010): Novel synthesis and characterization of nanosized y-Al_2O_3 from kaolin. J. Appl Clay Sci., 47: 438-443.

Yehia, A.A., Akelah, A.M., Rehab, A., El-Sabbagh, S.H., El Nashar, D.E., Koriem, A.A. (2012): Evaluation of clay hybrid nanocomposites of different chain length as reinforcing agent for natural and synthetic rubbers. J. Mater. & Des., 33:1-11.